African vulture optimizer algorithm based vector control induction motor drive system

Reham H. Mohammed[1], Ahmed M. Ismaiel[2], Basem E. Elnaghi[2], Mohamed E. Dessouki[3,4]
[1]Electrical Engineering Department, Faculty of Engineering, Suez Canal University, Ismailia, Egypt
[2]Electrical Power and Machines Department, Faculty of Engineering, Suez Canal University, Ismailia, Egypt
[3]Electrical Engineering Department, Faculty of Engineering, King Abdulaziz University, Rabigh, Saudi Arabia
[4]Electrical Engineering Department, Faculty of Engineering, Port Said University, Port Said, Egypt

Article Info

Article history:

Received Jul 30, 2022
Revised Sep 15, 2022
Accepted Oct 1, 2022

Keywords:

Adaptive fuzzy logic speed regulators
African vulture optimizer algorithm
Fuzzy like proportional differential
Induction motor variable speed drive

ABSTRACT

This study describes a new optimization approach for three-phase induction motor speed drive to minimize the integral square error for speed controller and improve the dynamic speed performance. The new proposed algorithm, African vulture optimizer algorithm (AVOA) optimizes internal controller parameters of a fuzzy like proportional differential (PD) speed controller. The AVOA is notable for its ease of implementation, minimal number of design parameters, high convergence speed, and low computing burden. This study compares fuzzy-like PD speed controllers optimized with AVOA to adaptive fuzzy logic speed regulators, fuzzy-like PD optimized with genetic algorithm (GA), and proportional integral (PI) speed regulators optimized with AVOA to provide speed control for an induction motor drive system. The drive system is simulated using MATLAB/Simulink and laboratory prototype is implemented using DSP-DS1104 board. The results demonstrate that the suggested fuzzy-like PD speed controller optimized with AVOA, with a speed steady state error performance of 0.5% compared to the adaptive fuzzy logic speed regulator's 0.7%, is the optimum alternative for speed controller. The results clarify the effectiveness of the controllers based on fuzzy like PD speed controller optimized with AVOA for each performance index as it provides lower overshoot, lowers rising time, and high dynamic response.

Corresponding Author:

Mohamed E. Dessouki
Department of Electrical Engineering, Faculty of Engineering, King Abdulaziz University
Rabigh 21911, Saudi Arabia
Email: dessouky_m@yahoo.com

1. INTRODUCTION

Induction motors are utilized in both residential and business settings. Air conditioners, washers, dryers, fans, freezers, pumps, and other similar devices make up the majority of these applications. The influence of these types of motors on energy savings is proportional to their efficiency in converting electrical energy into mechanical energy. Constant speed drives are used in these motors, resulting in low efficiency and increased energy consumption. However, the need for energy savings in electrical equipment has resulted in the usage of adjustable speed drives (ASDs) across all motor power ranges. By boosting speed rage and decreasing rotor inertia, a combination of changeable speed drives and control techniques may be employed to obtain improved performance [1], [2].

The field-oriented control was initially done for high-performance motor applications that are needed to work easily over the maximum speed, create full torque at zero speed, and have a high dynamic response including very rapid deceleration and acceleration. However, because of the field oriented control (FOC's) smaller motor, lower cost, and reduced power consumption, it also becomes more and more appealing for lesser performance applications [3]. In field orientation, the motor input currents are specified to make a specific angle between fluxes produced in the rotor and stator windings in a way that follows the direct current (DC) motor operation. The results are comparable to the dynamic response of a DC machine when the dynamic formulas for an induction motor are converted using well-known rotational transformation methods into a reference frame that changes with rotor flux. As with a DC machine's field current and armature current, this enables the induction motor stator current to be divided into a flux-producing component and a torque-producing component. The way to field-oriented control is information on the rotor transition position edge regarding the stator. Given that other motor characteristics are known, it is possible to register the edge using shaft position data [4]. Instead of applying three-phase currents to an induction motor, two perpendicular currents can be used to control the motor more easily. The motor's flux component and torque component are produced by these two currents, which are known as direct current (i_d) and quadrature current (i_q) respectively. The transition between a stationary reference frame and a reference frame, which is rotating synchronously with the stator flux, becomes then the problem. This leads us to the concept of reference frames. The concept of a reference frame is to represent an amount that is sinusoidal in one reference frame, to a constant value in a reference frame, which is rotating at the same speed as the rotating flux. Once a sinusoidal quantity is transformed to a constant value by careful choice of reference frame, it ends up conceivable to control that amount with conventional proportional-integral controllers.

Zeb *et al.* [5] present a smart control system for induction motors (IM) using an adaptive fuzzy logic controller (AFLC) based on the Levenberg-Marquardt algorithm which has an integral square error of 2.986 and compared the results to a conventional proportional integral (PI) speed controller. Several optimization algorithms were proposed for tuning the fuzzy logic controllers in many engineering applications, such as the genetic algorithm [6], grey-wolf optimizer [7], whale-optimization algorithm [8], and intelligent-based fuzzy methods such as the fuzzy logic controller [9], fuzzy-genetic controller [10], swarm-optimization and pattern search-based fuzzy controller [11], and differential-evolution-based fuzzy controller [12], which are applied to tune the PI controllers gain used in several power applications. Moreover, metaheuristic techniques such as the cuckoo-search algorithm [13], particle swarm optimization (PSO) [14], particle swarm optimization-sine-cosine based swarm optimization (PSO-SCSO) [15], and bees algorithm [16] are viable options for fine-tuning the settings of fuzzy logic controllers. All of these studies have offered novel methods for speed controller optimization, however they do so with relatively high integral square errors and slow convergence.

The African vultures optimization algorithm (AVOA), a brand-new metaheuristic algorithm inspired by nature, was put forth by Mirjalili and his associates in August 2021 [17]. It has more inclusive exploration and exploitation mechanisms. The usage of a random approach enhances the exploration and exploitation abilities of both mechanisms. This approach can ensure that the AVOA will not only skip a local optimum and have quick convergence but also guarantee that it is not too divergent [18]. To correctly design the fuzzy-like proportional differential (PD) speed controller for stability enhancement of speed performance, this paper provides a novel AVOA method. The induction motor is examined under various mechanical loading. The control methodology for these Visual Studio codes (VSCs) for PI and fuzzy-like PD speed controllers have been suitably adjusted by the AVOA. At a quick convergence speed, the AVOA algorithm adjusts the gains of PI and fuzzy-like PD speed controllers used in the system. The speed error is used as the objective function in a simulation-based optimization strategy.

2. METHOD

2.1. Field oriented control

Field-oriented control describes an induction machine in a *dq* coordinate system, with the d axis aligned with rotor flux and the *q* axis aligned with electromagnetic torque. The current, voltage, and flux of the motor can be analyzed in terms of space vector [19].

$$i_s = i_a + i_b e^{j\frac{2\pi}{3}} + i_c e^{j\frac{4\pi}{3}} \tag{1}$$

where (a, b, c) is the three-phase system domain. It must be transformed into a two-time variant coordinate system. Using a transformation matrix, we first transform (a, b, c) into (α, β) and then transform (α, β) into (d, q). The transformation matrix for transforming (a, b, c) into (α, β) is given in (2). The transformation matrix for (α, β) into (d, q) can be found in (3). Figure 1 shows the relation between the two domains:

$$i_{\alpha\beta o} = \frac{2}{3} * \begin{bmatrix} 1 & -\frac{1}{2} & -\frac{1}{2} \\ 0 & \frac{\sqrt{3}}{2} & -\frac{\sqrt{3}}{2} \\ \frac{1}{2} & \frac{1}{2} & \frac{1}{2} \end{bmatrix} \tag{2}$$

$$i_{dqo} = \frac{2}{3} * \begin{bmatrix} cos\theta & \cos\left(\theta - \frac{2\pi}{3}\right) & \cos\left(\theta + \frac{2\pi}{3}\right) \\ sin\theta & \sin\left(\theta - \frac{2\pi}{3}\right) & \sin\left(\theta + \frac{2\pi}{3}\right) \\ \frac{1}{2} & \frac{1}{2} & \frac{1}{2} \end{bmatrix} \tag{3}$$

where, θ is the position of the rotor flux. The flux and torque current components are estimated by (4)-(5):

$$i_{sd} = i_{s\alpha} cos\theta + i_{s\beta} sin\theta \tag{4}$$

$$i_{sq} = -i_{s\alpha} sin\theta + i_{s\beta} cos\theta \tag{5}$$

These values rely on the current vector (α, β) components and the flux position in the rotor; if the flux position becomes known exactly using position sensor then, by this projection, the (d, q) components can be estimated [19].

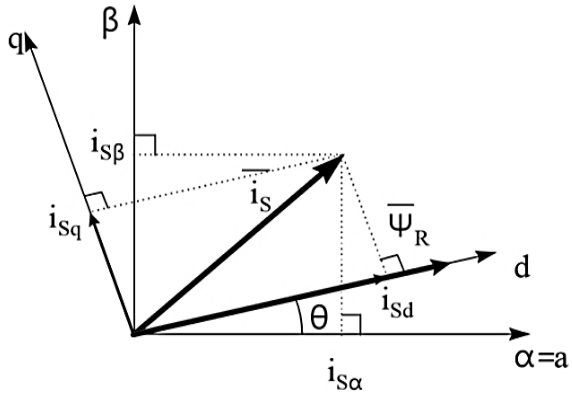

Figure 1. Stator current vector and its components in (α, β) and (d, q) domain

2.2. Speed controller

2.2.1. Proportional integral speed regulator

The control law for this technique is:

$$\mathrm{T} = K_p * \mathrm{e} + K_i * \int \mathrm{e}\, \mathrm{dt} \tag{6}$$

$$\mathrm{e} = \omega^* - \omega \tag{7}$$

where ω and ω^* are the actual and reference speed respectively. The controller output is controlled by PI speed regulator gains (K_p and K_i) that follow a set of principles to provide optimum control performance even when parameter volatility and drive nonlinearity are present. The high value of the error is amplified across the PI regulator in starting mode, resulting in considerable variances in the required torque. If the K_p and K_i values of the PI speed regulator surpass a specific threshold, the required torque fluctuates too much, destabilizing the system [20], [21]. To solve this problem, a limiter is used after the PI regulator. This limiter, when properly adjusted, keeps the speed error within limits, resulting in smooth variations in the necessary torque even when the PI speed regulator gains are relatively significant [22]. Figure 2 shows the block diagram for the PI controller. The K_p and K_i values of the PI speed regulator have been estimated using AVOA.

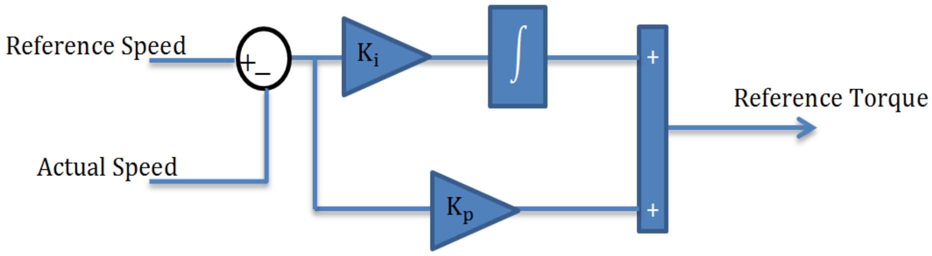

Figure 2. Block diagram of PI speed regulator

2.2.2. Adaptive fuzzy logic regulator

Adaptive control, as shown in Figure 3, is a fuzzy regulator with adjustable properties that change in response to system changes, such as output scaling factor, fuzzy rule, and membership function. It can improve the performance of nonlinear and complex speed control systems with variable torque-speed profiles [23]. A Sugeno-type fuzzy inference system (FIS) with two inputs (e, Δe) and one output (T_e^*) is used to simulate this regulator model, with the proportional value to change in speed added. As a result of this addition, the rising time (tr) will be even shorter. Adaptive fuzzy logic controller parameters are evaluated using Levenberg-Marquardt algorithm [5], [24].

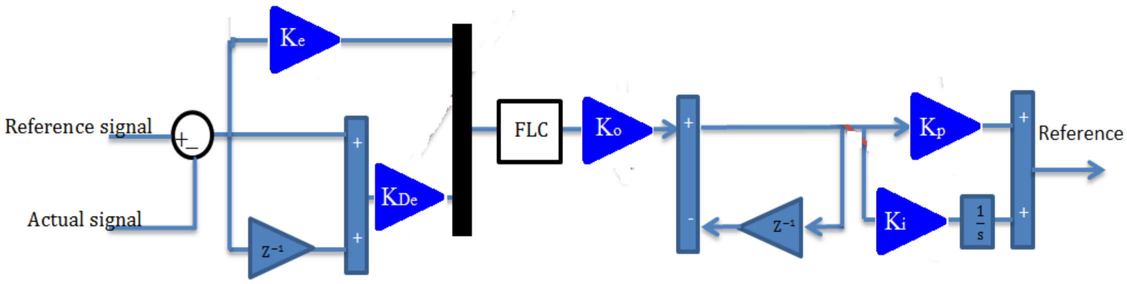

Figure 3. Block diagram of the adaptive fuzzy logic speed regulator

2.2.3. Fuzzy like PD regulator

It is discovered that the fuzzy-like PD technique is substantially more efficient. Non-linearizes with the individual's expertise and expert knowledge of the process to be regulated while constructing the regulator. Compared to traditional linear regulators, this method improves the system's performance, dependability, and resilience [25], [26]. Figure 4 depicts the Block diagram model of a fuzzy-like PD regulator. The model is built using gain coefficients *Kp*, *Kd*, and *Ko* that are set to 30, 40, and 100 respectively which have been estimated using AVOA. This regulator model is simulated using a Sugeno-type FIS with two inputs the error "e" in (6), the change in error "Δe" in (7) and one output (T_e^*) [27], [28].

$$\Delta e = e_k - e_{k-1} \tag{7}$$

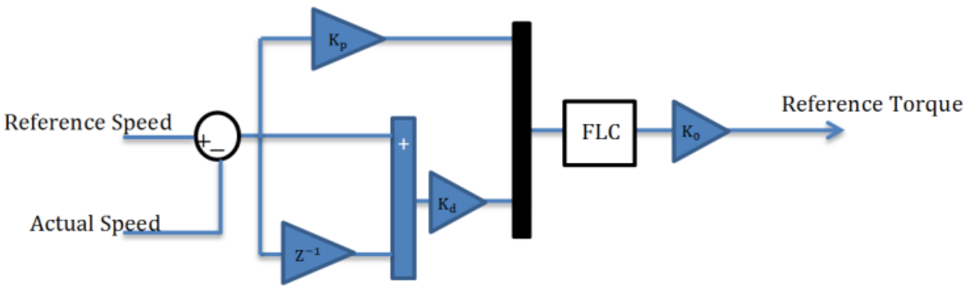

Figure 4. Block diagram of fuzzy like PD speed regulator

3. PROPOSED ALGORITHMS

3.1. African vulture optimizer algorithms

Costa *et al.* [16] presented the AVOA, a brand-new metaheuristic algorithm that draws inspiration from nature. Based on the aforementioned four criteria, the AVOA technique may be divided into five stages to imitate the behavior of different vultures during the foraging stage.

a) Population grouping: The best solution is identified as the best and the first vulture in this phase, the second solution is identified as the second-best vulture using (8), and the remaining vultures are assigned to the third group based on the second criteria. This phase follows the formation of the initial population [17].

$$R(i) = \begin{cases} BV_1 \; if \; p_i = Z_1 \\ BV_2 \; if \; p_i = Z_2 \end{cases} \tag{8}$$

where, BV_1 represents the best vulture, BV_2 represents the second-best vulture, $Z_1$and Z_2 are two random values in the range of [0,1], and their total is 1. The (9) is used to determine p_i, which was achieved with the roulette-wheel method.

$$p_i = \frac{F_i}{\sum_{i=1}^{l} F_i} \tag{9}$$

where, F_i represents the fitness of the first and second two vultures' groups. l is the total vultures number in each group.

b) The rate of starvation of vultures: When a flock of vultures does not need food, they have the stamina to go farther in search of it, but when they are, they are unable to keep up their long-distance flight. The hungry vultures will act aggressively as a result. Thus, vulture exploration and exploitation stages might be designed using this behavior. The F_i of the i^{th} vulture at the iteration is evaluated by (10).

$$F_i = (2 \times rand_i + 1) \times z \times \left(1 - \frac{iter_i}{iter_{\mathrm{m}}}\right) + t \tag{10}$$

where, F_i stands for vultures have had their fill, $rand_i$ is variable with a random value between 0 and 1. z stands for random number in the range of [-1, 1] which varies each iteration, t is determined by (11):

$$t = h \times (\sin^w \left(\frac{\pi}{2} \times \frac{iter_i}{iter_{\mathrm{m}}}\right) + \cos^w \left(\frac{\pi}{2} \times \frac{iter_i}{iter_{\mathrm{m}}}\right) - 1) \tag{11}$$

where, the chance of the vultures performing the exploration stage is given by the value of w, which is determined in advance. $iter_i$ stands for the current iteration number. $iter_{\mathrm{m}}$ is the total iterations, and h is random variable between -2 and 2. The (10) states that as the number of repetitions rises, F_i will steadily decrease. When the value of $|F_i|$ exceeds 1, the vultures begin the exploration stage and look for fresh food in various places. Otherwise, vultures enter the stage of exploitation and start searching the nearby area for richer meals.

c) Exploration stage: Due to their excellent vision in the environment, vultures can swiftly locate food and identify dead animals. However, because they spend a lot of time surveying their environment before flying great distances in search of food, vultures may have trouble finding food. Vultures in the AVOA can inspect various random locations using two distinct strategies, and a parameter named P_1in the range of [0, 1] is used to get either strategy. To choose one of the strategies during the exploration phase, a random number $rand_{p1}$ between 0 and 1 is utilized. The (19) is used if the value of $rand_i \leq P_1$, otherwise (13) is employed:

$$P(i+1) = R(i) - D(i) \times F_i \tag{12}$$

$$P(i+1) = R(i) - F_i + rand_2 \times ((ub - lb) \times rand_3 + lb) \tag{13}$$

where, $R(i)$ stands for one of the best vultures chosen in the current iteration with (8). $rand_2$ is a random number between 0 and 1, and lb and ub are the variables' lower and upper bounds, respectively. To increase the variety and search for different search space areas, $rand_3$ is used to give a high random coefficient at the search environment scale. The (14) determines $D(i)$ which represents the distance between the vulture and the current optimum one.

$$D(i) = |X \times R(i) - P(i)| \tag{14}$$

where, X is a random value between 0 and 2.

d) Exploitation: The AVOA's efficiency stage is now being investigated. The initial phase of exploitation is started by the AVOA. If $|F_i|$ is less than 1. P_2 in the range of [0,1] is utilized to decide which strategy is chosen. $rand_{p2}$ is a random number between 0 and 1 produced. The siege-fight strategy is applied slowly if this $rand_{p2} \geq P_2$. Otherwise, the rotational flying technique is used. The (15) illustrates this procedure.

$$P(i+1) = \begin{cases} D(i) \times (F_i + rand_4) - d(t) & if\ P_2 \geq rand_{p2} \\ R(i) - S_1 - S_2 & if\ P_2 < rand_{p2} \end{cases} \tag{15}$$

The distance $d(t)$ between the vulture and one of the two groups' best vultures, as computed by (16).

$$d(i) = R(i) - P(i) \tag{16}$$

$S_1$and S_2 are determined with (17) and (18), respectively:

$$S_1 = R(i) \times (\frac{rand_5 \times P(i)}{2\pi}) \times \cos\,(P(i)) \tag{17}$$

$$S_1 = R(i) \times (\frac{rand_6 \times P(i)}{2\pi}) \times sin\,(P(i)) \tag{18}$$

where, $rand_4, rand_5$ and $rand_6$ are random numbers between 0 and 1.

e) Exploitation: If $|F_i|$ is smaller than 0.5. $rand_3$ is a random number between 0 and 1. So if $P_3 \geq rand_3$. The goal of the method is to get different kinds of vultures to congregate around the food supply and engage in competition. The (19) may be used to update the vulture's location as a result.

$$P(i+1) = \frac{A_1 + A_2}{2} \tag{19}$$

where, $A_1$and A_2 are given by

$$A_1 = BV_1(i) - \frac{BV_1(i) \times P(i)}{BV_1(i) - (P(i))^2} \times F_i \tag{20}$$

$$A_2 = BV_1(i) - \frac{BV_2(i) \times P(i)}{BV_2(i) - (P(i))^2} \times F_i \tag{21}$$

The vultures would also congregate around the best vulture to scavenge the remaining food while the AVOA is in its second stage. The (22) can be used to update the vultures' location.

$$P(i+1) = R(i) - |d(t)| \times F_i \times Levy(d) \tag{22}$$

Lévy flight (LF) patterns were used to improve the AVOA's performance. These patterns were created using (23).

$$LF(x) = 0.001 \times \frac{u \times \sigma}{|v|^{\frac{1}{\beta}}} \tag{24}$$

$$\sigma = \left(\frac{\Gamma(1+\beta) \times \sin\left(\frac{\pi\beta}{2}\right)}{\Gamma(1+\beta^2) \times \beta \times 2 \times \left(\frac{\beta-1}{2}\right)} \right)^{\frac{1}{\beta}} \tag{25}$$

where, v and u are random numbers between 0 and 1, respectively, and β is a constant number of 1.5.

3.2. Genetic algorithm

The genetic algorithm (GA) is an effective iterative approach that uses benchmarks to reliably find the best solution to a range of engineering problems [29], [30]. The GA is predicated on the notion of "survival of the fittest". The first step is to produce at random a population of chromosomes. Once the random population has been reached, it is possible to evaluate the solution that was used for each string. The rank fitness scaling is employed in this work to avoid early convergence. Other evolutionary biology-inspired techniques used by the GA include natural selection, reproduction, mutation, and crossover. The method is applied using the uniform selection strategy, which has an extremely low spread and no bias [31].

The convergence of the fitness functions for the AVOA and GA is shown in Figure 5, where a slight change is seen after 300 iterations. To ensure that AVOA will work for the majority of runs since it is a stochastic optimization, the average optimized fitness function of integral square error (ISE) and the corresponding standard deviation for forty independent runs are generated, displayed, and compared as illustrated for PI speed regulator using AVOA, and fuzzy like PD speed regulator using both AVOA and GA in the Table 1. Fuzzy like PD speed regulator using AVOA achieves improvement by 92.6% in the average integral square error as compared to fuzzy-like PD speed regulator using GA and improvement by 71.13% when compared to PI under AVOA. It is important to emphasize that the AVOA's low standard deviations demonstrate its stability. Table 2 explains the maximum gains for fuzzy like PDs and PI speed regulators.

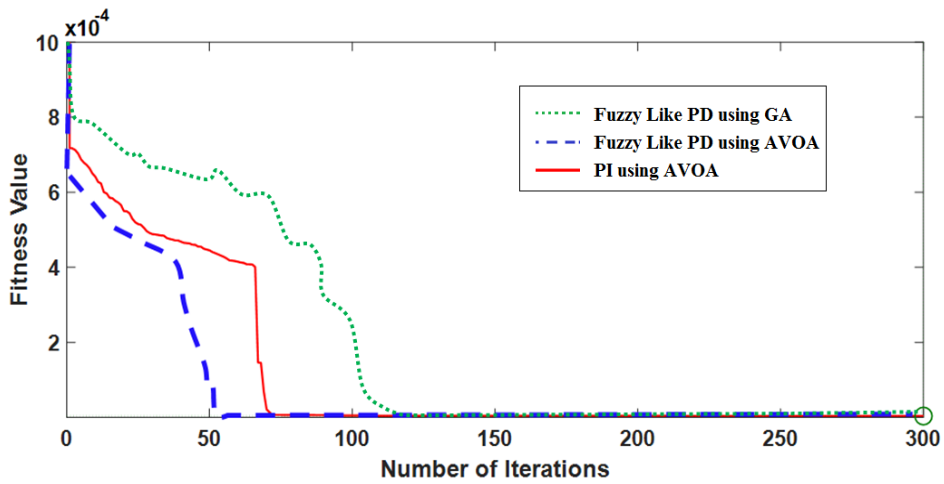

Figure 5. Cost convergence over iterations

Table 1. Comparison of the statistical results of used algorithms

Technique	Ave.	Std. dev.
Tuning using AVOA for PI speed regulator	0. 814	0.0435
Tuning using AVOA for Fuzzy like PD speed regulator	0. 235	0.0042
Tuning using GA for Fuzzy like PD speed regulator	3.174	0.0456

Table 2. Optimum parameters for speed regulator

Technique	Parameters
PI speed regulators optimized with AVOA	Kp=50.679 Ki=40.250
Fuzzy like PD speed regulators optimized with AVOA	Kp=30 Kd=40 Ko=100
Fuzzy like PD speed regulators optimized with GA	Kp=27.63 Kd=36.87 Ko=105

4. RESULTS AND DISCUSSION

To study the behavior of the studied control techniques, the simulation has been performed on two different induction motors (large-scale induction motor and small-scale induction motor). large-scale induction motor is examined utilizing MATLAB/Simulink under adaptive fuzzy logic controller, PI using AVOA, fuzzy PD-like using AVOA, and fuzzy PD-like using GA. A laboratory prototype of the control system is built using the DSPACE-DS1104 control board for a small induction motor, and the results are compared to those obtained using MATLAB/Simulink for the same motor in order to validate the suggested algorithm.

4.1. Large scale induction motor

The drive system for a three-phase, 20 HP, 380 V, two pair poles, 50 Hz induction motor is simulated using MATLAB/Simulink. We measure the speed for 2 sec for each studied control technique. The results of output speed at no load by using an Adaptive fuzzy logic controller, PI speed regulator with AVOA, fuzzy PD-like using both AVOA and GA are shown in Figure 6. The dynamic performance analysis with different mechanical loads (0, 20, and 30 N.m) is shown in Figure 6 and summarized in Table 3. It is noted that, at no load, the overshoot peak value of speed using Adaptive fuzzy logic controller is 7.6 rad/s while it is 3.7 rad/s by using PI speed regulator with AVOA, on other hand, it is 3.3 rad/s by employing fuzzy PD-like with AVOA and 8.6 rad/s by using fuzzy PD-like with GA. The fuzzy PD-like using AVOA and the PI using AVOA have less rising time and settling time than the adaptive fuzzy logic controller. The AVOA parameters show a fast dynamic response as compared to GA parameters for the same fuzzy-like PD parameters.

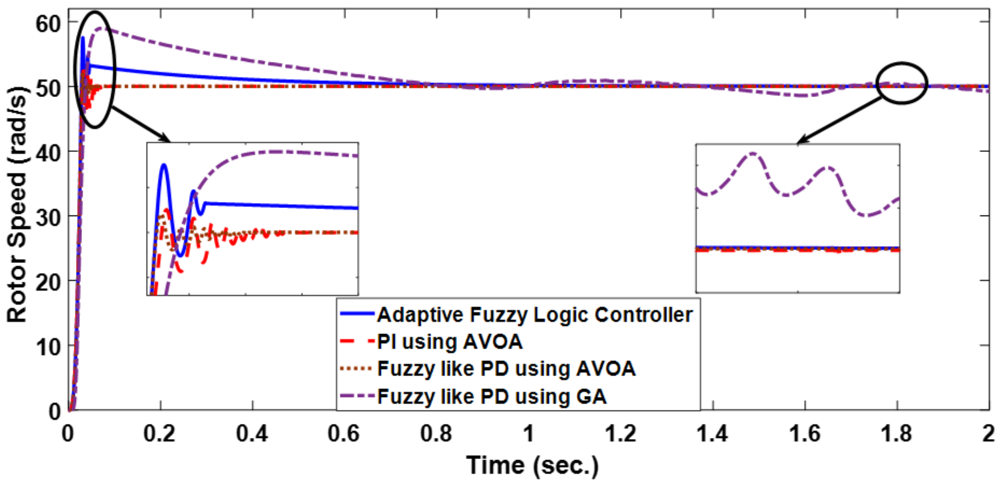

Figure 6. Simulation of motor speed for a reference speed of 50 rad/s and no-load

Table 3. Performance analysis of different speed controllers at different loads

Load (N.m)	Method	Tr (msec)	Mp (rad/s)	Ts (msec)
	Adaptive Fuzzy Logic Controller	20.337	7.6	530.2
No-load	PI speed regulator with AVOA Fuzzy	20.807	3.7	133.2
	PD-like using AVOA	20.327	3.3	98.6
	Fuzzy PD-like using GA	21.213	8.6	825.8
	Adaptive Fuzzy Logic Controller	19.161	5.6	432.6
20	PI speed regulator with AVOA Fuzzy	20.184	3.5	103.6
	PD-like using AVOA	19.177	3.3	89.02
	Fuzzy PD-like using GA	21.051	7.1	526.1
	Adaptive Fuzzy Logic Controller	19.203	5.3	326.4
30	PI speed regulator with AVOA Fuzzy	20.184	3	97.8
	PD-like using AVOA	19.100	2.8	82.31
	Fuzzy PD-like using GA	20.876	6.7	496.9

Figure 7 shows the electromagnetic torque produced under the examined control techniques. In comparison to other methods, it is discovered that the adaptive fuzzy logic speed controller in Figure 7(a) has very promising results with a low steady-state torque ripple of 2%, but it also has very high transient peak torque (-162 to 232 N.m). In contrast, the PI speed regulator with AVOA in Figure 7(b) has a significant disadvantage with a higher steady state torque ripple of 10.1%. As opposed to an adaptive fuzzy logic speed controller, fuzzy PD-like with AVOA shown in Figure 7(c) has a very low steady-state torque ripple of 1.9% and reduces the transient peak torque by 10.91%. From Figures 7(c) and 7(d), AVOA shows a very low steady-state torque ripple and reduces the transient peak torque as compared to GA. Table 4 illustrates how ISE is used to further assess the performance of the controller. The results reveal that the performance of the fuzzy like PD and PI speed regulator tested with AVOA is significantly superior to AFLC and conventional PI.

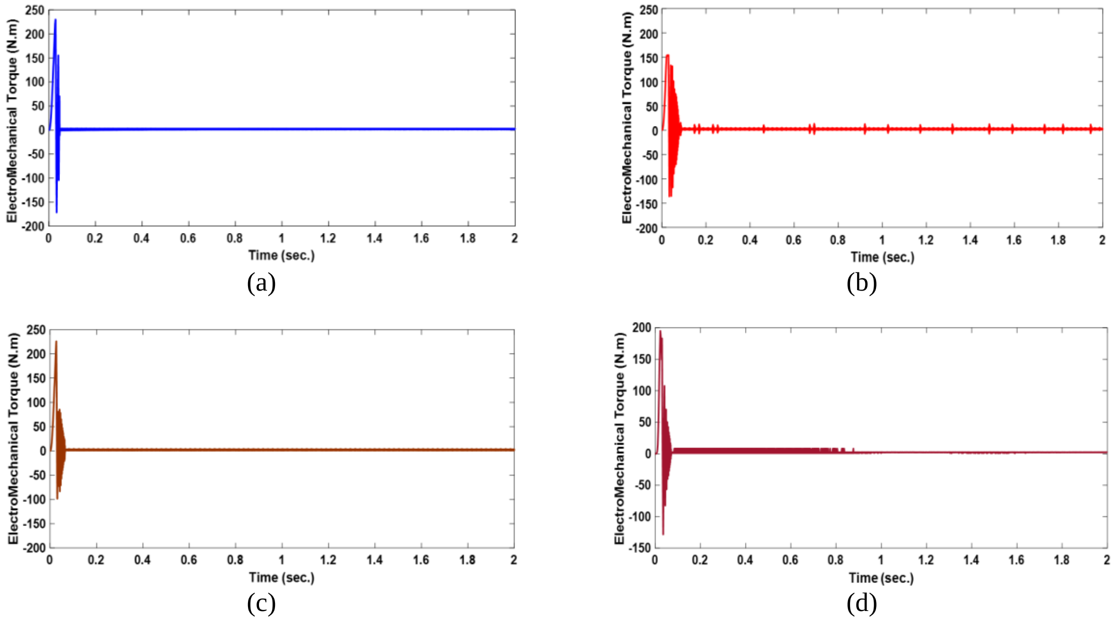

Figure 7. Simulation of the electromechanical torque for the reference speed 50 rad/s and no-load using (a) adaptive fuzzy logic controller, (b) PI speed regulator with AVOA, (c) fuzzy PD-like using AVOA, and (d) fuzzy PD-like using GA

Table 4. Integral square error performance at no-load

Method	ISE
Conventional PI	37.61
Adaptive Fuzzy Logic Controller	2.986
PI speed regulator with AVOA Fuzzy	0. 814
Fuzzy PD-like using AVOA	0. 235
Fuzzy PD-like using GA	3.174

4.2. Small scale induction motor

The MATLAB/Simulink platform is used to simulate the performance of the control system under fuzzy PD-like conditions of AVOA and GA in order to study their behaviors. A laboratory prototype of the control system is constructed using the DSPACE-DS1104 control board for a small induction motor (4-poles, 0.8 kW, 50 Hz, 230/400 V, cosφ 1/0.75, 3.2/2 Amp) to evaluate the simulation results and verify the viability of the suggested controller. A picture of the actual experimental system is shown in Figure 8.

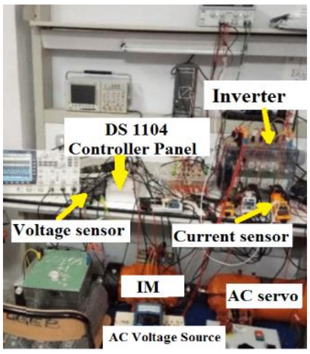

Figure 8. The actual laboratory setup of the system

Figures 9(a)-(b) and 10(a)-(b) display the simulation and experimental findings of the motor speed under fuzzy PD-like using GA and AVOA, respectively, at a command speed of 50 rad/s. Both Simulation and experimental results confirm that the fuzzy PD-like using AVOA has less rising time and settling time than the fuzzy PD-like using GA. The AVOA parameters exhibit a quick dynamic response as compared to GA parameters for the same fuzzy-like PD parameters.

Figures 11(a)-(b) and 12(a)-(b) display the simulation and experimental findings of the motor developed torque under fuzzy PD-like using GA and AVOA, respectively, at no-load and a command speed of 50 rad/s. Both Simulink and experimental results confirm that AVOA has a much lower steady-state torque ripple than GA and minimizes the transient peak torque. In addition, AVOA settles more quickly than GA.

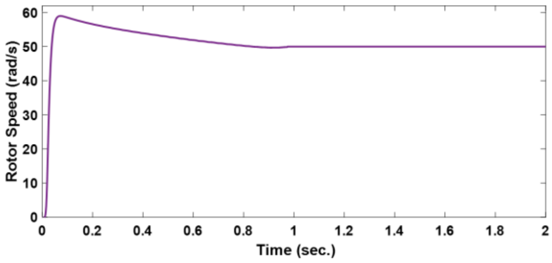

(a)

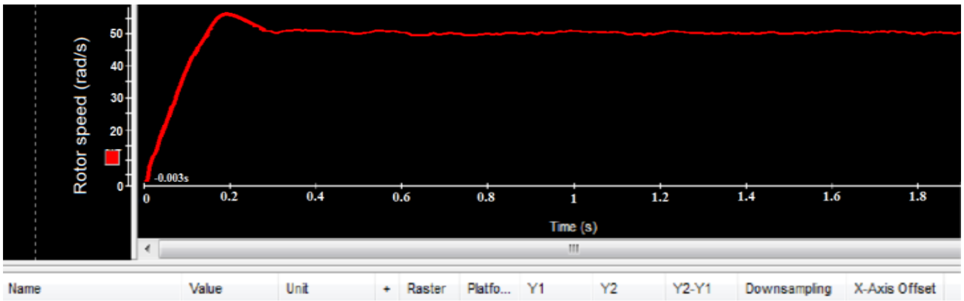

(b)

Figure 9. Simulation and experimental motor speed at no-load and command speed of 50 rad/s using fuzzy like PD with GA, (a) simulation and (b) experimental

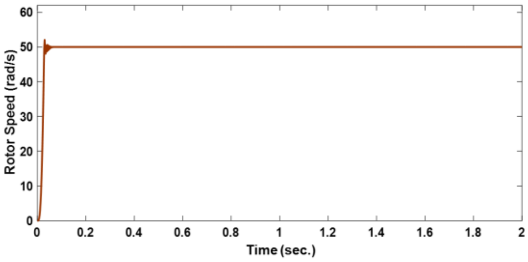

(a)

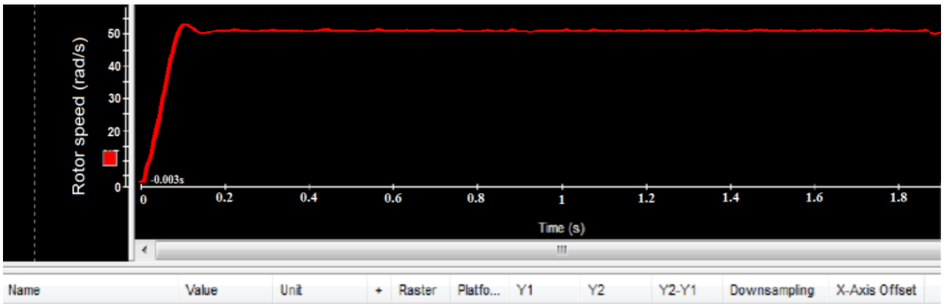

(b)

Figure 10. Simulation and experimental motor speed at no-load and command speed of 50 rad/s using fuzzy like PD with AVOA, (a) simulation and (b) experimental

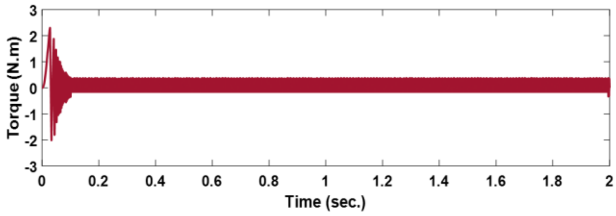

(a)

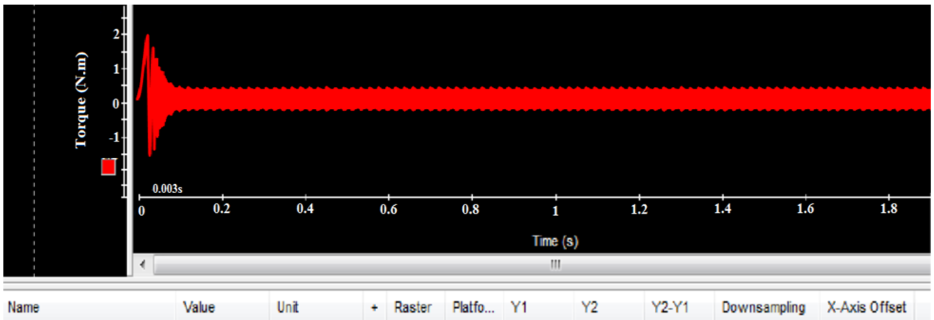

(b)

Figure 11. Simulation and experimental motor developed torque at no-load and command speed of 50 rad/s using fuzzy like PD with GA, (a) simulation and (b) experimental

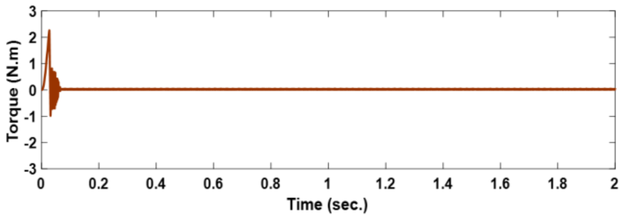

(a)

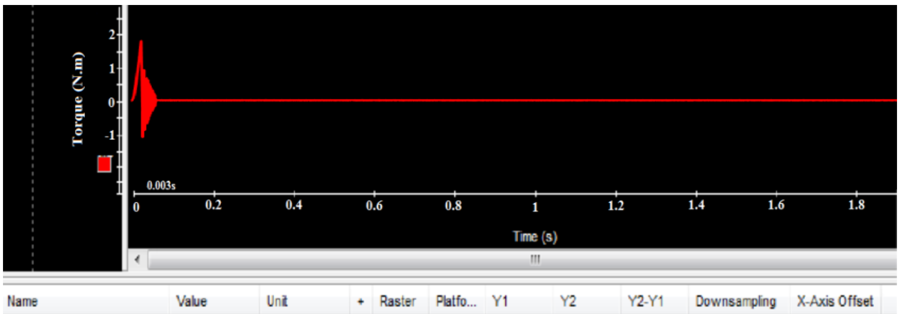

(b)

Figure 12. Simulation and experimental motor developed torque at no-load and command speed of 50 rad/s using fuzzy like PD with AVOA, (a) simulation, (b) experimental

5. CONCLUSION

Using four different control methods, including an adaptive fuzzy logic controller, a PI speed regulator with AVOA, fuzzy PD-like with GA, and fuzzy PD-like with AVOA, a three-phase induction motor speed control drive system is investigated. The motor speed is regulated based on the integral square speed error and the change in this error. The newly proposed AVOA technique is appealing due to its clear formulation and simplicity of implementation. The performance of the induction motor drive system under the investigated control approaches is examined using MATLAB/Simulink. The simulation results demonstrate that using fuzzy-like PD with AVOA technique outperforms in terms of the performance and convergence rate. In the fuzzy-like PD speed regulator, the AVOA reduced the maximum peak overshoot for speed dynamic response by 61.65% and the rising time by 4.17% as compared to GA. A quick response, outstanding anti-interference, and tracking precision are all advantages. Consequently, the AVOA technique is the most effective method for determining the tuning parameters that offer the optimal speed dynamic response (rising time, peak overshoot, and settling time). The applicability, effectiveness, and superiority of the AVOA to identify the optimal solution have been demonstrated.

To assess the simulation findings and confirm the viability of the proposed controller, a lab prototype of the control system is built utilizing the dSPACE DS1104 control board. Experimental and simulation results indicate that the AVOA outperforms the GA in terms of overshoot and steady-state torque ripple. Using fuzzy PD-like with AVOA or PI speed regulator with AVOA as speed controller makes them a very good option compared to the adaptive fuzzy logic controller or fuzzy PD-like using GA.

REFERENCES

[1] F. Wang, Z. Zhang, X. Mei, J. Rodríguez, and R. Kennel, "Advanced control strategies of induction machine: field oriented control, direct torque control and model predictive control," *Energies*, vol. 11, no. 1, Jan. 2018, doi: 10.3390/en11010120.

[2] L. Yan and X. Song, "Design and implementation of Lemberger model-based predictive torque control of induction machine for robustness improvement," *IEEE Transactions on Power Electronics*, vol. 35, no. 3, pp. 2257–2262, Mar. 2020, doi: 10.1109/TPEL.2019.2939283.

[3] F. B. Motto, R. Tchuidjan, B. Ndzana, and C. T. Tchinda, "The characteristic of control algorithms for an induction electromotor by the parameters change in stator winding voltage," *European Journal of Engineering Research and Science*, vol. 4, no. 4, pp. 48–51, Apr. 2019, doi: 10.24018/ejers.2019.4.4.1226.

[4] L. Zhen and L. Xu, "Fuzzy learning enhanced speed control of an indirect field-oriented induction machine drive," *IEEE Transactions on Control Systems Technology*, vol. 8, no. 2, pp. 270–278, Mar. 2000, doi: 10.1109/87.826798.

[5] K. Zeb, Z. Ali, K. Saleem, W. Uddin, M. A. Javed, and N. Christofides, "Indirect field-oriented control of induction motor drive based on adaptive fuzzy logic controller," *Electrical Engineering*, vol. 99, no. 3, pp. 803–815, Sep. 2017, doi: 10.1007/s00202-016-0447-5.

[6] H. M. Hasanien and S. M. Muyeen, "Design optimization of controller parameters used in variable speed wind energy conversion system by genetic algorithms," *IEEE Transactions on Sustainable Energy*, vol. 3, no. 2, pp. 200–208, Apr. 2012, doi: 10.1109/TSTE.2012.2182784.

[7] M. H. Qais, H. M. Hasanien, and S. Alghuwainem, "Augmented grey wolf optimizer for grid-connected PMSG-based wind energy conversion systems," *Applied Soft Computing*, vol. 69, pp. 504–515, Aug. 2018, doi: 10.1016/j.asoc.2018.05.006.

[8] H. M. Hasanien, "Performance improvement of photovoltaic power systems using an optimal control strategy based on whale optimization algorithm," *Electric Power Systems Research*, vol. 157, pp. 168–176, Apr. 2018, doi: 10.1016/j.epsr.2017.12.019.

[9] P. Zambrana-Lopez, J. Fernández-Quijano, J. J. Fernandez-Lozano, A. Garcia-Cerezo, and P. M. M. Rubio, "Fuzzy logic tuning of a PI controller to improve the performance of a wind turbine on a semi-submersible platform under different wind scenarios," *IFAC-PapersOnLine*, vol. 53, no. 2, pp. 12364–12371, 2020, doi: 10.1016/j.ifacol.2020.12.1243.

[10] S. Ustun and M. Demirtas, "Optimal tuning of PI coefficients by using fuzzy-genetic for V/f controlled induction motor," *Expert Systems with Applications*, vol. 34, no. 4, pp. 2714–2720, May 2008, doi: 10.1016/j.eswa.2007.05.029.

[11] R. K. Sahu, S. Panda, and G. T. C. Sekhar, "A novel hybrid PSO-PS optimized fuzzy PI controller for AGC in multi area interconnected power systems," *International Journal of Electrical Power and Energy Systems*, vol. 64, pp. 880–893, Jan. 2015, doi: 10.1016/j.ijepes.2014.08.021.

[12] M. Abedini, E. Mahmodi, M. Mousavi, and I. Chaharmahali, "A novel fuzzy PI controller for improving autonomous network by considering uncertainty," *Sustainable Energy, Grids and Networks*, vol. 18, Jun. 2019, doi: 10.1016/j.segan.2019.100200.

[13] R. N. Kalaam, S. M. Muyeen, A. Al-Durra, H. M. Hasanien, and K. Al-Wahedi, "Optimisation of controller parameters for grid-tied photovoltaic system at faulty network using artificial neural network-based cuckoo search algorithm," *IET Renewable Power Generation*, vol. 11, no. 12, pp. 1517–1526, Oct. 2017, doi: 10.1049/iet-rpg.2017.0040.

[14] J. Zhao, M. Lin, D. Xu, and L. Hao, "Vector control of hybrid axial field flux-switching permanent magnet machine based on particle swarm optimization," in *2015 IEEE Magnetics Conference (INTERMAG)*, May 2015, pp. 1–1, doi: 10.1109/INTMAG.2015.7157225.

[15] A. Taieb and A. Ferdjouni, "A New design of fuzzy logic controller optimized By PSO-SCSO applied To SFO-DTC induction motor drive," *International Journal of Electrical and Computer Engineering (IJECE)*, vol. 10, no. 6, pp. 5813–5823, Dec. 2020, doi: 10.11591/ijece.v10i6.pp5813-5823.

[16] B. L. G. Costa, V. D. Bacon, S. A. O. da Silva, and B. A. Angelico, "Tuning of a PI-MR controller based on differential evolution metaheuristic applied to the current control loop of a shunt-APF," *IEEE Transactions on Industrial Electronics*, vol. 64, no. 6, pp. 4751–4761, Jun. 2017, doi: 10.1109/TIE.2017.2674609.

[17] B. Abdollahzadeh, F. S. Gharehchopogh, and S. Mirjalili, "African vultures optimization algorithm: A new nature-inspired metaheuristic algorithm for global optimization problems," *Computers and Industrial Engineering*, vol. 158, Aug. 2021, doi: 10.1016/j.cie.2021.107408.

[18] J. Fan, Y. Li, and T. Wang, "An improved African vultures optimization algorithm based on tent chaotic mapping and time-varying mechanism," *Plos One*, vol. 16, no. 11, Nov. 2021, doi: 10.1371/journal.pone.0260725.

[19] B. M. Wilamowski and J. D. Irwin, Eds., *Power electronics and motor drives*. CRC Press, 2018.

[20] R. Marouane and Z. Malika, "Particle swarm optimization for tuning PI controller in FOC chain of induction motors," in *2018 4th International Conference on Optimization and Applications (ICOA)*, Apr. 2018, pp. 1–5, doi: 10.1109/ICOA.2018.8370512.

[21] J. Talla, V. Q. Leu, V. Smidl, and Z. Peroutka, "Adaptive speed control of induction motor drive with inaccurate model," *IEEE Transactions on Industrial Electronics*, vol. 65, no. 11, pp. 8532–8542, Nov. 2018, doi: 10.1109/TIE.2018.2811362.

[22] M. A. Hannan *et al.*, "Role of optimization algorithms based fuzzy controller in achieving induction motor performance enhancement," *Nature Communications*, vol. 11, no. 1, Dec. 2020, doi: 10.1038/s41467-020-17623-5.

[23] Y. Han, J. Yu, L. Zhao, H. Yu, and C. Lin, "Finite-time adaptive fuzzy control for induction motors with input saturation based on command filtering," *IET Control Theory and Applications*, vol. 12, no. 15, pp. 2148–2155, Oct. 2018, doi: 10.1049/iet-cta.2018.0011.

[24] A. Farhat and K. C. Cheok, "Improving adaptive network fuzzy inference system with Levenberg-Marquardt algorithm," in *2017 Annual IEEE International Systems Conference (SysCon)*, Apr. 2017, pp. 1–6, doi: 10.1109/SYSCON.2017.7934787.

[25] G. Boukhalfa, S. Belkacem, A. Chikhi, and S. Benaggoune, "Genetic algorithm and particle swarm optimization tuned fuzzy PID controller on direct torque control of dual star induction motor," *Journal of Central South University*, vol. 26, no. 7, pp. 1886–1896, Jul. 2019, doi: 10.1007/s11771-019-4142-3.
[26] A. Mishra, "Design of speed controller for squirrel-cage induction motor using fuzzy logic based techniques," *International Journal of Computer Applications*, vol. 58, no. 22, 2012.
[27] I. Ferdiansyah, M. R. Rusli, B. Praharsena, H. Toar, Ridwan, and E. Purwanto, "Speed control of three phase induction motor using indirect field oriented control based on real-time control system," in *2018 10th International Conference on Information Technology and Electrical Engineering (ICITEE)*, Jul. 2018, pp. 438–442, doi: 10.1109/ICITEED.2018.8534864.
[28] D. Driankov, H. Hellendoorn, and M. Reinfrank, *An introduction to fuzzy control*. Springer Science and Business Media, 2013.
[29] M. G. Bijan, M. Al-Badri, P. Pillay, and P. Angers, "Induction machine parameter range constraints in genetic algorithm based efficiency estimation techniques," *IEEE Transactions on Industry Applications*, vol. 54, no. 5, pp. 4186–4197, Sep. 2018, doi: 10.1109/TIA.2018.2836344.
[30] Z. Fazlipour, R. Kianinezhad, and M. Razaz, "Genetic algorithm based design optimization of a six phase induction motor," *Journal of Electrical Engineering and Technology*, vol. 10, no. 3, pp. 1007–1014, May 2015, doi: 10.5370/JEET.2015.10.3.1007.
[31] B. A. Avdeev and A. V Vyngra, "Simulation of variable frequency controlled ac induction motor operating on non-linear load," in *2020 IEEE Conference of Russian Young Researchers in Electrical and Electronic Engineering (EIConRus)*, Jan. 2020, pp. 2346–2349, doi: 10.1109/EIConRus49466.2020.9038963.

BIOGRAPHIES OF AUTHORS

Reham H. Mohammed was born on March 21, 1983. She received the B.Sc., M.Sc. degrees from faculty of engineering-Mansoura University in 2005 and 2010, respectively and Ph.D. degree from faculty of engineering-Suez Canal University in 2016. In 2005, she joined the Mansoura University, Faculty of engineer, in Egypt, as assistant Research. In 2011, she worked as assistant lecturer in Suez Canal University, faculty of engineer, in Egypt. Currently, she worked as lecturer at Suez Canal University, Faculty of Engineer, in Egypt. She has more than 16 scientific research papers published in prestigious international journals. She can be contacted at email: reham.elenani@eng.suez.edu.eg.

Ahmed M. Ismaiel was born on September 19, 1996. He received the B.Sc., M.Sc. degrees from faculty of engineering-Suez Canal University in 2019 and 2021, respectively. Currently, He works as assistant Lecturer in Electrical Power and Machine Engineering department, Suez Canal University, Ismailia, Egypt. He is interested in Automation Control, Renewable Energy, Motor Drive design and Vector control techniques, and DSP control and power electronics applications. He can be contacted at email: ahmed123ismaiel@gmail.com.

Basem E. Elnaghi received the B.Sc., M.Sc. and Ph.D. degrees in electrical power engineering in 2002 and 2009, and 2015 respectively, from Suez Canal University, Port Said, Egypt. Since 2015, he has been Associate professor with the electrical engineering Department, faculty of engineering, Suez Canal University. He joined the Department of faculty of engineering, Suez Canal University, Rabigh. His main professional interests include ac and dc drives, direct torque and field-oriented control techniques, and DSP control, control of electrical machines and wind energy conversion system, and power electronics applications. He can be contacted at email: Basem_elhady@eng.suez.edu.eg.

Mohamed E. Dessouki was born in Bohiera, Egypt in 1976. He received his B.Sc., M.sc. and Ph.D. degrees, from Faculty of Engineering, Suez Canal University in 1999, 2004 and 2010 respectively, all in Electrical Engineering. He joined the Department of Electrical Engineering, Faculty of Engineering, Suez Canal University as a demonstrator in 2000. Then, he became an assistant Lecturer from 2004 to 2010 and has been a Lecturer since 2010. He joined the Department of Electrical Engineering, King Abdulaziz University, Rabigh. His main professional interests include AC and DC drives, direct torque and field-oriented control techniques, and DSP control and power electronics applications. He can be contacted at email: dessouky_m@yahoo.com.